Available online at www.sciencedirect.com
SCIENCE DIRECT
Thin Solid Films 511–512 (2006) 587 – 592
thin solid films
www.elsevier.com/locate/tsf

Efficiency limiting morphological factors of MDMO-PPV:PCBM plastic solar cells

H. Hoppe [a,*], T. Glatzel [b], M. Niggemann [c], W. Schwinger [d], F. Schaeffler [d], A. Hinsch [c], M. Ch. Lux-Steiner [b], N.S. Sariciftci [a]

[a] Linz Institute for Organic Solar Cells (LIOS), Physical Chemistry, Johannes Kepler University Linz, Altenbergerstr. 69, A-4040 Linz, Austria
[b] Hahn-Meitner Institute, Solar Energy Research, Glienicker Str. 100, 14109 Berlin, Germany
[c] Fraunhofer Institute for Solar Energy Systems (ISE), Heidenhofstr. 2, D-79110 Freiburg, Germany
[d] Institut für Halbleiter-und Festkörperphysik, Johannes Kepler University Linz, Altenbergerstr. 69, A-4040 Linz, Austria

Available online 23 January 2006

Abstract

Fundamental aspects of the influence of the nanomorphology in phase-separated conjugated polymer/fullerene bulk heterojunction blends are presented. A variety of experimental techniques were combined to resolve the structure of fullerene and polymer domains on the nanometer scale. As predicted theoretically, it is experimentally identified that the phase-separated domain size as well as the percolation of both hole- and electron-conducting phases is crucial to improve the power conversion efficiency of organic solar cell devices. Among the experimental techniques we applied atomic force microscopy (AFM), Kelvin probe force microscopy (KPFM), scanning and transmission electron microscopy (SEM, TEM). New insights are presented about the conformation and distribution of the conjugated polymer within the photoactive layer, which has a major impact on the device performance.

Keywords: Organic; Photovoltaic; Morphology; Microscopy

1. Introduction

With the discovery of the photoinduced electron transfer between a soluble poly(*para*-phenylenevinylene) and the buckminsterfullerene C_{60} the development of organic solar cells based on polymer-fullerene heterojunctions has commenced [1,2]. In contrast to the rather well-defined material interface in bilayer structures, blending two constituents in the bulk heterojunction approach is a lot more demanding towards morphological requirements in the nano-regime [3]. Early morphological studies already revealed the built up of bicontinuous networks between the electron conducting fullerene and the hole transporting polymer phases [4]. It is comprehensible that in solid state blends bicontinuous networks allow the different charge carriers to reach their respective electrode.

Since the primary photoexcitations within these organic materials have a very limited diffusion length in the range of 10 nm, and since these excitons are only dissociated at the polymer–fullerene heterojunction interface, it becomes evident that the scale of phase separation in the blend should not exceed that length scale considerably. On the other hand, a too intimate mixing can limit the charge carrier transport properties, when percolation is thereby disabled. Thus, there is a tradeoff required between charge generation and undisturbed transport. In this report it will be shown that some minimum scale of phase separation is inherently present due to the conformation of the conjugated polymers.

The dramatic increase in power conversion efficiency from 0.9% to 2.5% due to change of the solvent from which the polymer–fullerene solution was spin cast, was assigned to changes in the morphology [5]. At that time and thereafter many efforts have been undertaken to deepen the understanding of the morphology for soluble PPV-derivative:fullerene blends [6–17]. Many of the past studies have been focused on the exploration of the fullerene phase in the blend nanostructure. With this work we would like to contribute some results concerning the polymer phase nanomorphology.

We have investigated blends of MDMO-PPV (poly[2-methoxy-5-(3,7-dimethyloctyloxy)]-1,4-phenylenevinylene) to-

* Corresponding author.
E-mail address: harald.hoppe@tu-ilmenau.de (H. Hoppe).

0040-6090/$ - see front matter © 2005 Elsevier B.V. All rights reserved.
doi:10.1016/j.tsf.2005.12.071

gether with the soluble fullerene C_{60}-derivative PCBM (1-(3-methoxycarbonyl) propyl-1-phenyl [6,6] C_{61}), spin cast from either toluene or chlorobenzene solutions. The combination of several investigation techniques capable to probe on the nanometer scale allows us to draw a conclusive picture of the molecular assembly within these photoactive blends.

2. Experimental

2.1. Materials

MDMO-PPV (poly-[2-(3,7-dimethyloctyloxy)-5-methyloxy]-*para*-phenylene-vinylene) with a molecular weight of about 10^6 (M_W 1.150.000 g/mol / M_N=170.000 g/mol) and a quoted glass transition temperature of about 65 °C was provided by Covion (Germany). PCBM (1-(3-methoxycarbonyl) propyl-1-phenyl [6,6]C_{61}) of purity better than 99.5% was purchased from J. C. Hummelen (Univ. of Groningen, The Netherlands). PEDOT:PSS (poly[3,4-(ethylenedioxy) thiophene]: poly(styrene sulfonate)) (Baytron P) was purchased from Bayer (Germany). ITO covered glass was purchased from MERCK (Germany).

2.2. Preparation

The organic films were prepared under ambient conditions or in an Argon glove box. PEDOT:PPS was spin cast from an aqueous solution with a concentration of 0.5% (wt.). All solutions were prepared by dissolving MDMO-PPV or PCBM or the two together in the respective solvent. The solutions were stirred overnight under ambient (for chlorobenzene) or slightly elevated (for toluene, 50 °C) temperatures, without any sonication or filtering. The photoactive films were prepared by spin casting from either toluene or chlorobenzene solutions of the blended materials onto glass or ITO-glass(/PEDOT:PSS) substrates.

2.3. Characterization

AFM measurements were performed with a Dimension 3100 system (Digital Instruments, Santa Barbara, US) in tapping mode. SEM measurements were performed using a Cold Field Emission scanning electron microscope Hitachi S-4700. TEM measurements were done with a JEOL 2011 FasTEM HR-TEM in bright field mode (at 100 keV). The UHV-KPFM measurements took place under ultra high vacuum in a modified Omicron UHV-scanning tunneling/atomic force microscope (at a pressure $p<10^{-10}$ mbar). Further experimental details can be found in Refs. [15,17,18].

3. Results and discussion

As a starting point the differences of MDMO-PPV:PCBM blend films are discussed on the base of SEM measurements. Fig. 1 shows the cross-sections of chlorobenzene and toluene cast blends. The chlorobenzene cast blend shows a rather smooth film structure including some brighter particles that can be assigned to the polymer phase [15]. The toluene cast blend exhibits some large (several hundred nanometers) lens shaped embeddings consisting of PCBM, which are surrounded by the polymer-rich matrix phase [15]. The contrast between the phases is somewhat reduced in this case, as the sputtered layer of platinum was thicker than for the chlorobenzene cast film.

With transmission electron microscopy (TEM) pristine films of MDMO-PPV and PCBM are easy distinguishable (compare Fig. 2): while for (2a) MDMO-PPV a completely amorphous diffraction signal was recorded, (2b) the PCBM films yielded diffraction fringes, typical of some short-range order that has been assigned earlier to a nanocrystalline phase of the fullerene [4,19]. For the chlorobenzene (2c) and toluene (2d) cast blend films of MDMO-PPV and PCBM the diffraction fringes are found on any place of the sample. Therefore it can be concluded that the matrix phase around the darker appearing PCBM clusters consists of a blend of MDMO-PPV and PCBM. Due to a thermal annealing step of 4 h at 150 °C the toluene cast blend (Fig. 2e) is driven to a more complete phase separation between the polymer and the fullerene: the PCBM organizes thereby into micron-sized large crystalline aggregates with even monocrystalline reflexes (lower inset). The former matrix phase is thereby diluted and now a completely amorphous electron diffraction signal is obtained between the large aggregates (upper inset). Thus it is proposed, that between the fullerene

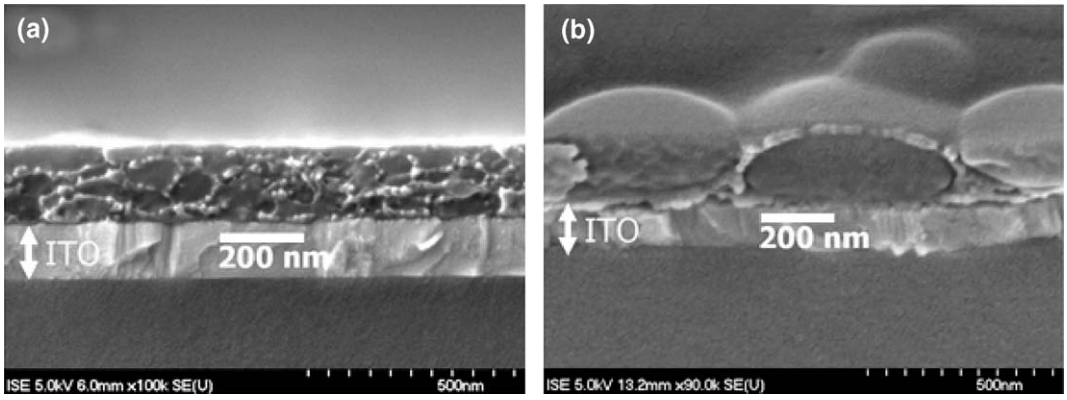

Fig. 1. SEM cross-section images of MDMO-PPV:PCBM blend films cast on ITO-glass from (a) chlorobenzene and (b) toluene solution. The brighter little objects are polymer nanospheres, whereas the large inclusion in (b) is a PCBM cluster.

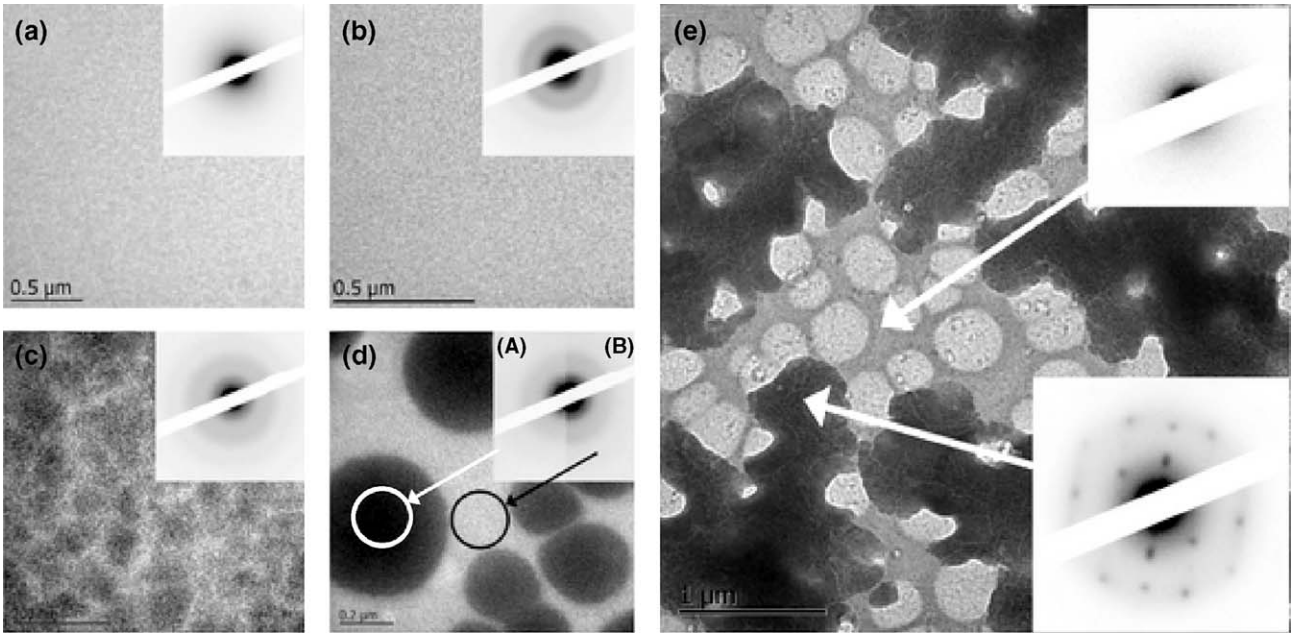

Fig. 2. TEM results on (A) MDMO-PPV, (B) PCBM, (C) chlorobenzene and (D) toluene based MDMO-PPV:PCBM blends. The color-inverted insets show the corresponding electron diffraction signals: MDMO-PPV appears amorphous, PCBM multi-crystalline (fringes). In the blends (C, D) fullerene fringes can be found on any place. Thermal annealing at 150 °C for 4 h drives the system into complete phase separation (E), causing the growth of single crystalline PCBM domains (dark large aggregates). Between the PCBM crystallites the remaining polymer is still present.

aggregates the bare polymer phase is present. On a closer look by tapping mode AFM measurements, again little spherical particles can be detected (compare Fig. 3b). These particles appear here slightly larger than in the SEM images, since the AFM-tip has a finite size and apex angle. For lower temperatures, the phase separation process is incomplete and thus parts of the fullerene clusters still remain at their original places (Fig. 3a). For temperatures higher than a certain barrier temperature (Fig. 3c) the remaining polymer phase is distorted considerably. The spherical shapes are not found anymore and it appears that the polymer matrix is molten. In addition, after the annealing step at 150 °C there was a considerable increase in the MDMO-PPV fluorescence observed [15], a confirmation for the remaining nearly fullerene-free polymer matrix as result of a coarse phase separation between the bare materials itself.

To provide further evidence for the coiled spherical conformation of the polymer, several polymer nanospheres were measured in magnifications of SEM images. Fig. 4 shows an example with a typical diameter of about 15 nm for the nanosphere. In the right side a visualization of the coiled polymer conformation is drawn for clarity. Taking a molecular mass of $m=10^6$ u, and a density of $\rho=910$ kg/m^3 [20] for MDMO-PPV, the volume of a single polymer chain becomes approximately $V_c=1.8\cdot10^{-24}$ m^3. For a sphere of the same volume the diameter calculates to ca. 15 nm, and an astonishing well agreement between the size of one nanosphere and the calculated volume taken up by a single MDMO-PPV chain is found. Note that varying the molecular weight between $2.5\cdot10^5$ and $2.5\cdot10^6$ u changes the resulting nanosphere diameter only between 10 to 20 nm.

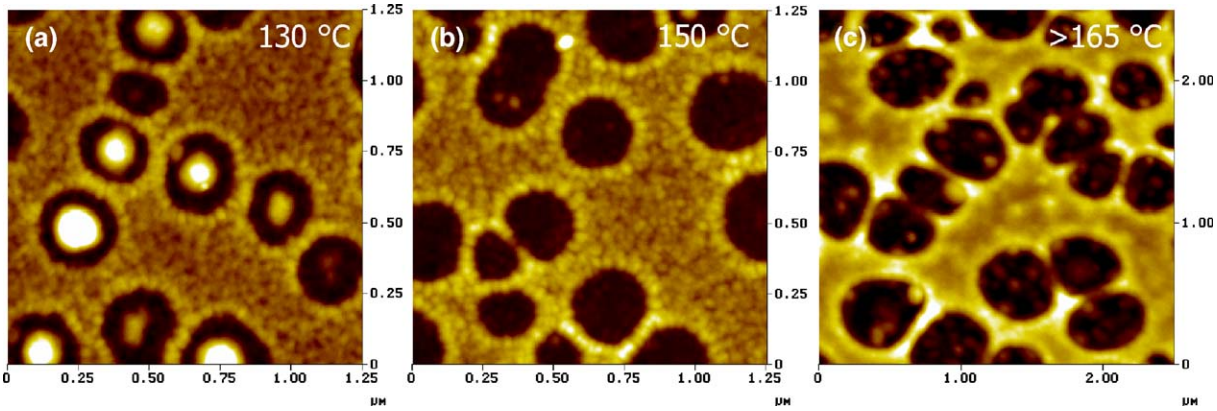

Fig. 3. The polymer-rich region between the PCBM crystallites imaged by tapping mode AFM measurements after thermal annealing for 4 h at different temperatures is shown. While up to 150 °C the polymer nanospheres can be detected, for temperatures larger than 165 °C these spheres are not visible anymore and the polymer has been molten.

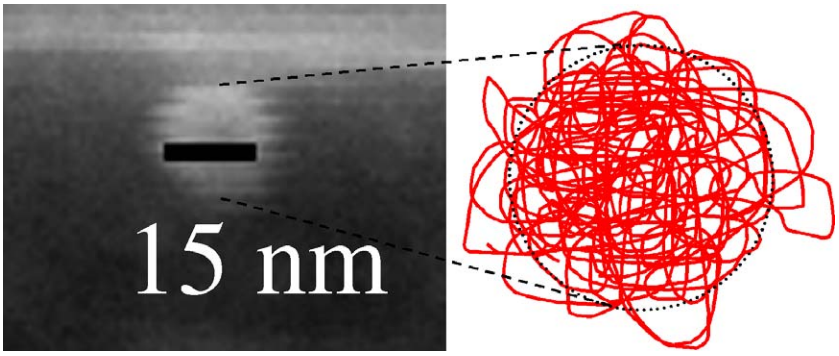

Fig. 4. Magnification of an SEM cross-sectional measurement: a polymer nanosphere has a typical radius of 15 nm in chlorobenzene based blends. The conformation of the polymer chain is illustrated in the right side.

Though for toluene cast blends some remaining fluorescence of the fullerene PCBM has been observed [15], the corresponding amount of singlet exciton recombinations is too small to explain a loss in the photocurrent of 50% and more as compared to chlorobenzene cast blend films. It can be therefore expected that the longer-lived triplet excitons are still able to reach the PCBM–MDMO-PPV interface at the surface of those lens shaped clusters and contribute to the charge generation process (compare with Ref. [21]). Furthermore, if the large size of the fullerene clusters would prevent the charge generation, it would be expected that the contribution of the PCBM absorption to the whole spectral photocurrent would be reduced in comparison to chlorobenzene based blends. This however has not been found, indeed the contributions of PCBM and MDMO-PPV absorption to the spectral photocurrent seems to be rather balanced [15]. Since both, charge generation and absorption are rather unaffected by the change of the spin casting solvent [5], the efficiency limiting bottleneck of toluene based MDMO-PPV:PCBM blends can be expected in the charge transport.

Using Kelvin probe force microscopy it is able to detect the local work function (and thus the position of the Fermi-level) spatially resolved. Pristine films of PCBM and MDMO-PPV exhibit similar values for the work function (around 4.4 eV), both in the dark and under 442 nm HeCd cw-laser illumination [17]. The situation is rather different for the two blend films: for chlorobenzene cast blends a very homogeneous distribution of the work function is found (~4.55 eV) compare Fig. 5b, d). Yet under illumination the work function value changes drastically and the work function is lowered by more than 300 meV (~4.2 eV, compare Fig. 6). For toluene cast blends the situation is almost reversed: first the topography and the work function are strongly correlated, second and especially under illumination the work function is increased up to 4.7 eV on top of the elevations caused by the PCBM-clusters (compare Fig. 7).

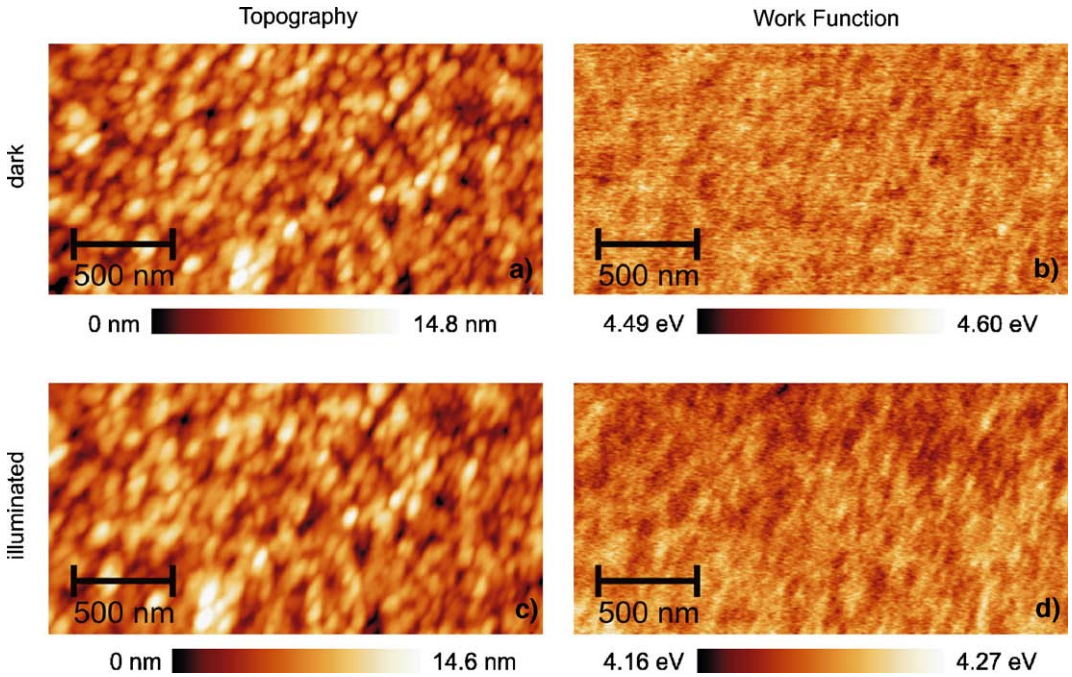

Fig. 5. KPFM results on chlorobenzene based blends. Shown are the topography (a, c) and the work function (b, d), in the dark (a, b) and under illumination (c, d). The work function is spatially very homogeneous. (Reproduced from Ref. [17] with permission, copyright 2005, American Chemical Society).

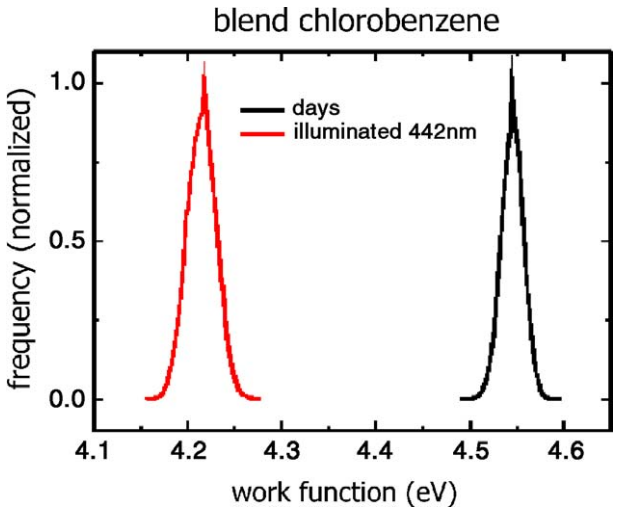

Fig. 6. Histogram of the work function distribution on chlorobenzene based MDMO-PPV:PCBM blends determined in the dark (centered around 4.55 eV) and under 442 nm cw HeCd laser illumination (centered around 4.2 eV).

How can these results be understood? Since the work function simply corresponds to the level of the Fermi energy, it is a measure for the electron density. Thus it can be concluded that the electron density is increased at the surface of chlorobenzene cast blends upon illumination. As the PCBM phase has access to the film surface (compare Fig. 1a), enrichment with electrons as a result of the charge generation based on the photoinduced charge transfer can explain the observed effect. For toluene cast blends on the other hand, since the fullerene clusters are embedded in a polymer-rich skin layer (compare with Fig. 1b and Ref. [15]), clearly the density of holes has to be increased near the surface upon illumination. Since in the solar cell configuration the electron extracting aluminium electrode is placed on top of the film surface, the electrons have to pass this hole-rich region and suffer parasitic recombination. For the holes the same consideration holds vice versa. It should be noted that due to the work function difference strong electric fields between the anode and the cathode dictate a rather vertical charge transport direction with respect to the surface plane at short circuit conditions, in contrast to the field effect transistor geometry. This may further force the encounter of electrons and holes. The situation between chlorobenzene and toluene cast films is summarized schematically in Fig. 8. In chlorobenzene cast blends (Fig. 8a), electrons and holes can access percolated pathways to reach the respective electrodes. In Fig. 8b the situation is depicted for an enclosed PCBM cluster as present in toluene cast blends: here electrons and holes will bump into each other, as the percolation is not

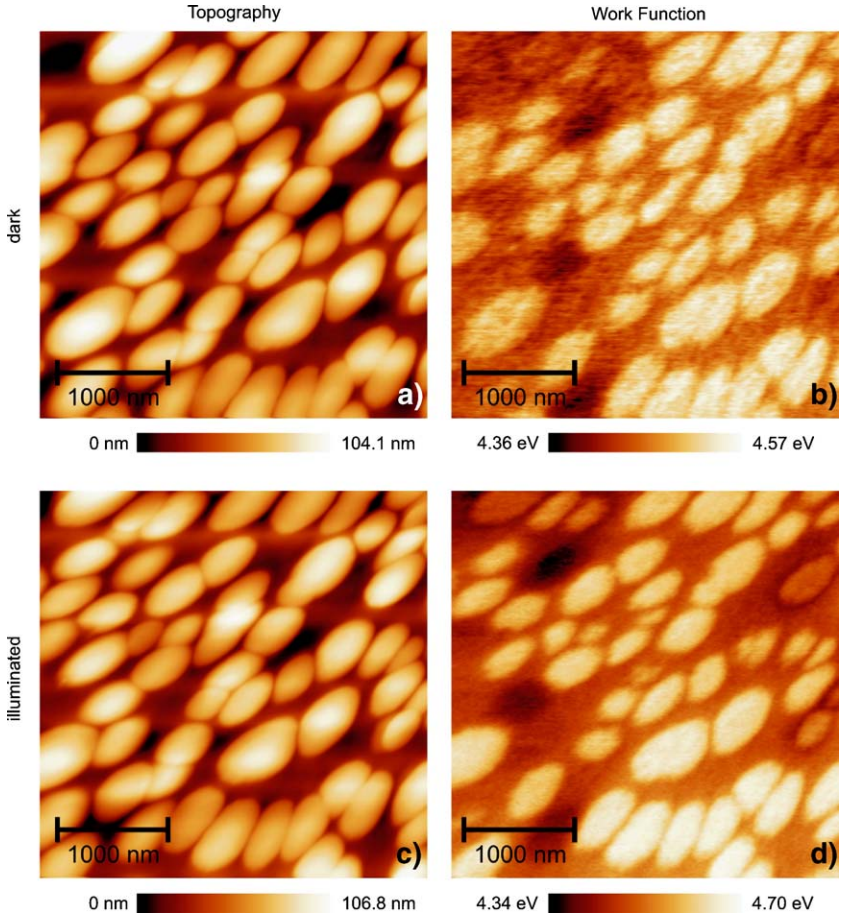

Fig. 7. KPFM results obtained for toluene cast MDMO-PPV:PCBM blend films. Shown are the topography (a, c) and the work function (b, d), in the dark (a, b) and under illumination (c, d). On top of the PCBM clusters the highest work functions are detected. (Reproduced from Ref. [17] with permission, copyright 2005, American Chemical Society).

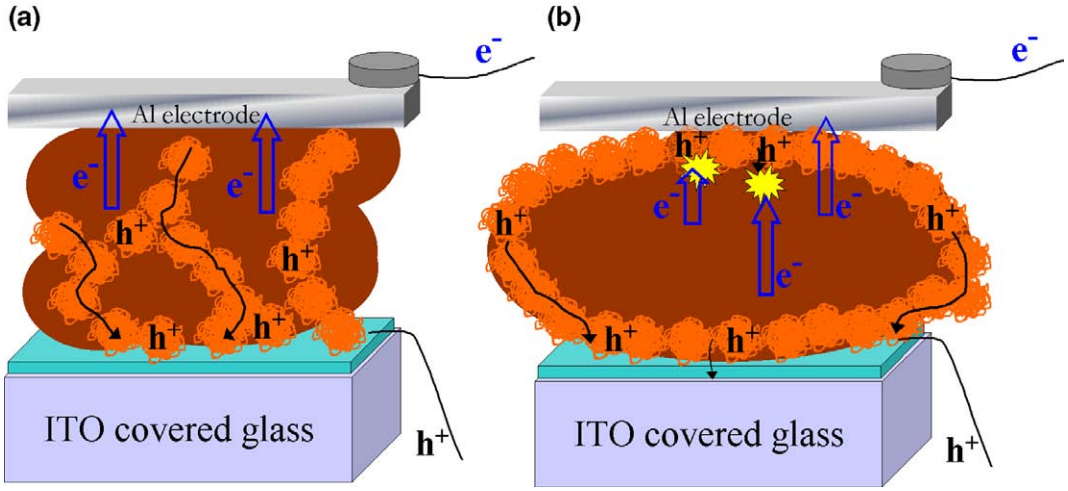

Fig. 8. Schematic of (a) chlorobenzene and (b) toluene cast MDMO-PPV:PCBM blend layers as active layer in the solar cell. In (a) holes and electrons find percolated pathways to reach the respective electrode. In (b) electrons and holes suffer recombination due to missing percolation.

sufficient. This parasitic recombination can now account for the large difference in the photocurrents observed between toluene and chlorobenzene cast blends. In addition, the reduced PCBM content in the polymer-rich matrix phase around the PCBM clusters might not offer appropriate conditions for charge transport either.

4. Conclusions

In summary, we have shown that a difference in the nanophase morphology is responsible for the different performances of MDMO-PPV:PCBM bulk heterojunction devices. As main loss mechanism for the photocurrent in toluene cast blend films a non-sufficient percolation of electron and hole conducting phases has been identified. The identification of the different phases was reached down to the molecular level, revealing that single MDMO-PPV polymer chains are present in the blends in a coiled conformation as nanosphere.

Acknowledgements

Financial support was partly provided by the German Ministry for Education and Research (BMBF, contract numbers 01SF0026 and 01SF0119). Part of this work was performed within the Christian Doppler Society's dedicated laboratory on Plastic Solar Cells co-funded by Konarka Corporation.

References

[1] N.S. Sariciftci, L. Smilowitz, A.J. Heeger, F. Wudl, Science 258 (1992) 1474.
[2] N.S. Sariciftci, D. Braun, C. Zhang, V.I. Srdanov, A.J. Heeger, G. Stucky, F. Wudl, Appl. Phys. Lett. 62 (1993) 585.
[3] G. Yu, J. Gao, J.C. Hummelen, F. Wudl, A.J. Heeger, Science 270 (1995) 1789.
[4] C.Y. Yang, A.J. Heeger, Synth. Met. 83 (1996) 85.
[5] S.E. Shaheen, C.J. Brabec, N.S. Sariciftci, F. Padinger, T. Fromherz, J.C. Hummelen, Appl. Phys. Lett. 78 (2001) 841.
[6] J. Liu, Y. Shi, Y. Yang, Adv. Funct. Mater. 11 (2001) 420.
[7] T. Martens, J. D'Haen, T. Munters, L. Goris, Z. Beelen, J. Manca, M. D'Olieslaeger, D. Vanderzande, L.D. Schepper, R. Andriessen, The influence of the microstructure upon the photovoltaic performance of MDMOPPV:PCBM bulk hetero-junction organic solar cells, in: G.E. Jabour, S.A. Carter, J. Kido, S.T. Lee, N.S. Sariciftci (Eds.), Organic and Polymeric Materials and Devices — Optical, Electrical, and Optoelectric Properties, Mater. Res. Soc. Symp. Proc., vol. 725, Warrendale, PA, 2002, 7.11.1.
[8] T. Martens, J. D'Haen, T. Munters, Z. Beelen, L. Goris, J. Manca, M. D'Olieslaeger, D. Vanderzande, L.D. Schepper, R. Andriessen, Synth. Met. 138 (2003) 243.
[9] T. Martens, Z. Beelen, J. D'Haen, T. Munters, L. Goris, J. Manca, M. D'Olieslaeger, D. Vanderzande, L.D. Schepper, R. Andriessen, Morphology of MDMO-PPV:PCBM bulk hetero-junction organic solar cells studied by AFM, KFM and TEM, in: Z.H. Kafafi, D. Fichou (Eds.), Organic Photovoltaics III, Proceedings of SPIE, vol. 4801, SPIE, Bellingham, WA, 2003, p. 40.
[10] M.T. Rispens, A. Meetsma, R. Rittberger, C.J. Brabec, N.S. Sariciftci, J.C. Hummelen, Chem. Commun. 17 (2003) 2116.
[11] M.M. Wienk, J.M. Kroon, W.J.H. Verhees, J. Knol, J.C. Hummelen, P.A. van Hall, R.A.J. Janssen, Angew. Chem. Int. Ed. 42 (2003) 3371.
[12] C.R. McNeill, H. Frohne, J.L. Holdsworth, J.E. Furst, B.V. King, P.C. Dastoor, Nano Lett. 4 (2004) 219.
[13] X. Yang, J.K.J. van Duren, R.A.J. Janssen, M.A.J. Michels, J. Loos, Macromolecules 37 (2004) 2151.
[14] J.K.J. van Duren, X. Yang, J. Loos, C.W.T. Bulle-Lieuwma, A.B. Sieval, J.C. Hummelen, R.A.J. Janssen, Adv. Funct. Mater. 14 (2004) 425.
[15] H. Hoppe, M. Niggemann, C. Winder, J. Kraut, R. Hiesgen, A. Hinsch, D. Meissner, N.S. Sariciftci, Adv. Funct. Mater. 14 (2004) 1005.
[16] C.R. McNeill, H. Frohne, J.L. Holdsworth, P.C. Dastoor, Synth. Met. 147 (2004) 101.
[17] H. Hoppe, T. Glatzel, M. Niggemann, A. Hinsch, M.C. Lux-Steiner, N.S. Sariciftci, Nano Lett. 5 (2005) 269.
[18] H. Hoppe, M. Drees, W. Schwinger, F. Schäffler, and N.S. Sariciftci, Synth. Met. 152 (2005) 117.
[19] X. Yang, J.K.J. van Duren, M.T. Rispens, J.C. Hummelen, R.A.J. Janssen, M.A.J. Michels, J. Loos, Adv. Mater. 16 (2004) 802.
[20] C.W.T. Bulle-Lieuwma, W.J.H.v. Gennip, J.K.J.V. Duren, P. Jonkheijm, R.A.J. Janssen, J.W. Niemantsverdriet, Appl. Surf. Sci. 203–204 (2003) 547.
[21] P. Peumans, A. Yakimov, S.R. Forrest, J. Appl. Phys. 93 (2003) 3693.